Hindawi
Journal of Nanomaterials
Volume 2020, Article ID 8958043, 14 pages
https://doi.org/10.1155/2020/8958043

Research Article

Preparation and Characterization of Rare Earth-Doped Ti/SnO_2-Sb-Mn Electrodes for the Electrocatalytic Performance

Thet Phyo Wai, Yilin Yin, Xiao Zhang, and Zenghe Li

Beijing Key Laboratory of Environmentally Harmful Chemical Analysis, College of Chemistry, Beijing University of Chemical Technology, Beijing 100029, China

Correspondence should be addressed to Zenghe Li; lizh@mail.buct.edu.cn

Received 19 January 2020; Accepted 4 April 2020; Published 16 May 2020

Guest Editor: Tetiana Dontsova

The modified Ti/SnO_2-Sb-Mn/Re electrodes were prepared using rare earth (Re) Gd, Eu, Ce, and Er and various molar ratios of tin and manganese by thermal decomposition. To investigate the electrocatalytic performance of electrodes, phenol was applied as a model pollutant. Phenol removal pursued pseudofirst-order kinetics in the experimental range. The experimental outcomes show that the phenol degradation at ~95% and ~97% was found in Mn (1 mol%)/Re and Mn (2 mol%)/Re electrodes after treatment for 140 min. Accelerated lifetime testing showed that the best-accelerated service life could be measured only in Mn (3 mol%)/Re and Mn (4 mol%)/Re compared with other prepared Mn (0%,1%, and 2%)/Re electrodes under the condition of 500 $mAcm^{-2}$ current density in this study. The modified electrodes were then characterized, including oxygen evolution potential (OEP), crystal structure, and surface composition of the electrode coatings.

1. Introduction

Industrial wastewater has been causing genuine ecological and medical issues [1], and this problem cannot be solved by conventional procedures [2]. Various methods are applied to treat wastewater relying upon its purpose, including filtration [3], ultrasonic oxidation [4], biological treatments [5, 6], adsorption [7], coagulation [8], electrocoagulation [9], and electroflotation [10]. Regardless, these methodologies have a few drawbacks, for example, high living arrangement time required, utilization of explicit and costly chemicals, solid waste generation, and in some cases low effectiveness.

Electrochemical oxidation procedure stands apart as a clean innovation that creates modest quantities of squanders, being exceptionally reproducible and effectively controllable and permitting mechanization and moderately minimized plants of simple establishment [11, 12]. The stability and electrocatalytic properties of the anodic material was advanced with the development of dimensionally stable anodes (DSA), in which a metallic base of Ti is covered with some metal oxides, for example, RuO_2, TiO_2, and SnO_2, among others [13, 14]. DSA show high electroactive zones because of their mud-split morphology, permitting the direct oxidation of organic pollutants on the electrode surface at low possibilities, and can advance the development of active intermediates to play out the indirect oxidation of pollutants [15]. The exhibition of a DSA is essentially impacted by the electrode material [16]. PbO_2 [17], IrO_2 [18], RuO_2 [19], and SnO_2 [20] have high oxygen overvoltage. Of these, the metal oxides SnO_2 and PbO_2 are believed to be unrivaled for the oxidation of phenol. SnO_2 as a promising material and an n-type semiconductor has high oxygen overpotential; a suitable amount of Sb consistently is doped to improve the conductivity just as an electrocatalytic activity [21]. Including an interlayer, Ti/Sb-SnO_2/PbO_2 [22, 23], Ti/Sb-SnO_2/MnO_x [24], and Ti/IrO_2/Sb-SnO_2 [25], significantly draw out the service life of a Ti/Sb-SnO_2 electrode [21]. The degradation efficiency is also reduced at different degrees.

Including an interlayer, Mn-doped Sb-SnO_2 between the substrate and the Sb-SnO_2 covering can enormously

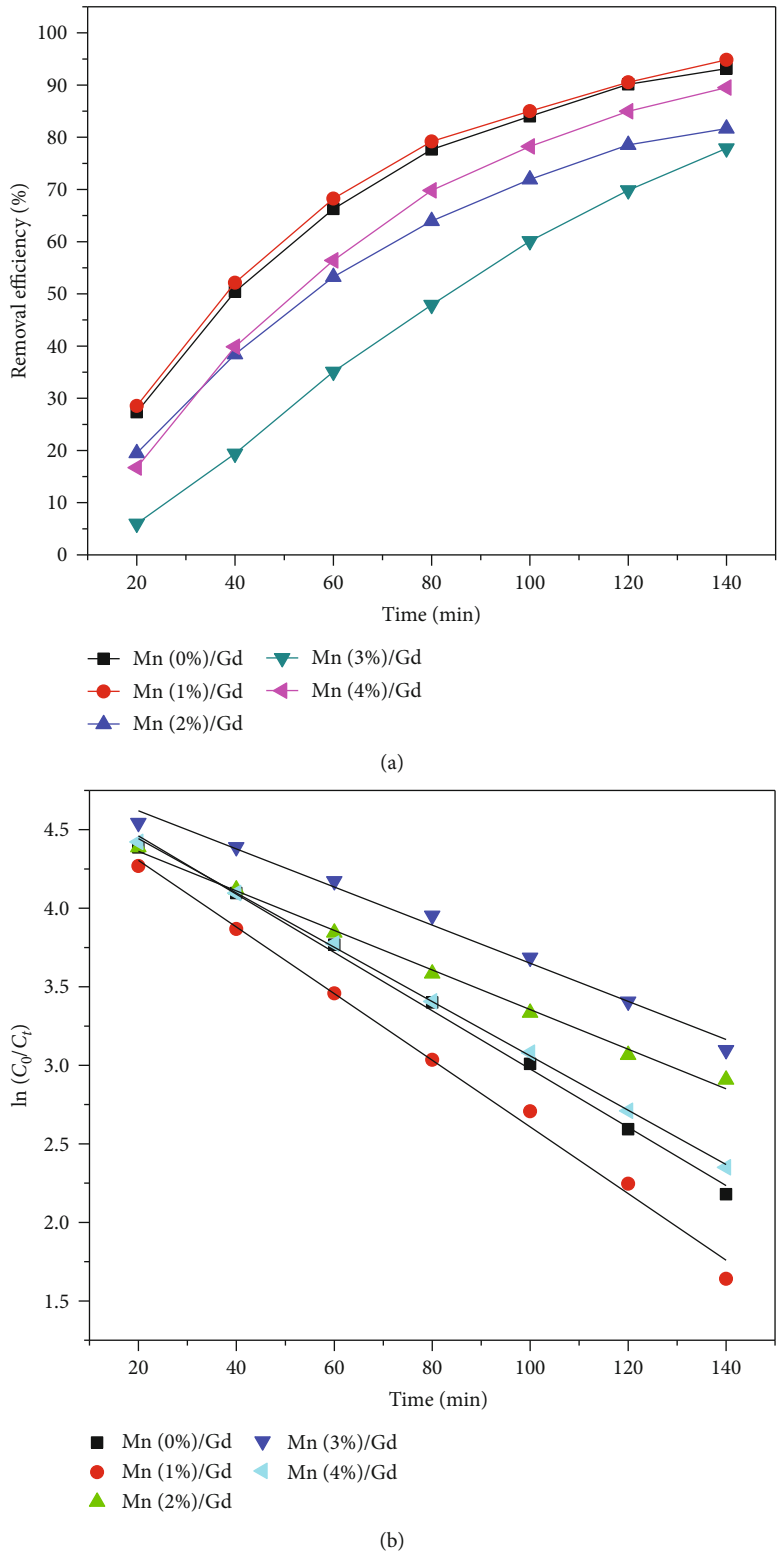

Figure 1: Electrochemical degradation performance of phenol with Ti/Mn-Sb-SnO_2/Gd electrodes modified with various Mn contents. (a) Removal efficiency. (b) Kinetic analysis of the curves.

build the service life of the electrode [26, 27]. Rare earth has been exhibited to upgrade chemical catalytic processes by either acting as powerful oxidants or helping catalytic processes such as purification of vehicle exhaust gas [28–30]. The addition of some rare earth elements can enhance the electrocatalytic performance of the Ti/Sb-SnO_2 electrode [31]. In the present research, the Ti/SnO_2-Sb-Mn/Re electrodes were prepared with

Table 1: Kinetic parameters of phenol in electrochemical processes by Ti/Mn-Sb-SnO_2/Re electrodes (Gd and Eu) modified with various Mn contents.

	Mn (0%)/Gd	Mn (1%)/Gd	Mn (2%)/Gd	Mn (3%)/Gd	Mn (4%)/Gd
Rate constants (k) (min^{-1})	0.0197	0.0212	0.0126	0.0121	0.0173
R^2	0.9990	0.9942	0.9964	0.9898	0.9995
	Mn (0%)/Eu	Mn (1%)/Eu	Mn (2%)/Eu	Mn (3%)/Eu	Mn (4%)/Eu
Rate constants (k) (min^{-1})	0.0165	0.0209	0.0164	0.0195	0.0148
R^2	0.9964	0.9948	0.9821	0.9926	0.9861

different tin/manganese molar ratios and four kinds of rare earth (Re) Gd, Eu, Ce, and Er by thermal decomposition. And their electrochemical performance was evaluated based on the degradation of phenol.

The modified electrodes were then characterized including X-ray diffraction (XRD), scanning electron microscopy (SEM), an energy dispersive spectroscopy (EDS), and cyclic voltammetry (CV) techniques.

2. Experimental

2.1. Titanium Sheet Surface Treatment. The dimensions of titanium sheets (20 mm × 50 mm × 0.5 mm, >99.6 purity, BaoTi Co. Ltd., China) were polished thoroughly with 320-grit abrasive papers. Then, they were degreased with mixed solution of acetone and 1 mol·L^{-1} NaOH (v/v 1 : 1) by the use of ultrasonic bath for 30 min After removing solid impurities and grease, they were subsequently etched in 10% oxalic acid at 98°C for 2 h to result in active rough surface on the Ti sheets. At last, they were thoroughly washed with deionized water. The pretreated Ti substrates lost their metallic sheen and were gray in color.

2.2. Preparation of SnO_2-Sb-Mn Intermediate Layer. The interlayer was coated on the pretreated Ti sheets by the thermal decomposition method [20]. In the intermediate layer coating solution, 17.5 g $SnCl_4{\cdot}5H_2O$ (98%, Sigma Aldrich), 0.570 g $SbCl_3$ (99.5%, Merck), and Mn $(NO_3)_2$ (molar ratios of Sn/Mn of 100 : 0, 100 : 1, 100 : 2, 100 : 3, and 100 : 4, respectively) were dissolved into 50 ml isopropanol with 2.5 ml hydrochloric acid. The pretreated Ti sheets were dipped in the coating solution and dried at 120°C for 5 min to evaporate the solvents. The dipping and drying were repeated 5 times, and the Ti sheets were heated at 550°C in a muffle oven for 20 min. After dipping, drying and heating were repeated 3 times and the electrodes were finally annealed at 550°C for 2 h.

2.3. Preparation of Rare Earth Outer Layer. For the outer layer coating solution, 17.5 g $SnCl_4{\cdot}5H_2O$, 0.570 g $SbCl_3$, 2.5 ml of concentrated (37%) HCl, and proper rare earth nitrates (molar ratio of Re/Sn of 2 : 100) were prepared in 50 ml isopropanol. The electrodes coated with Mn layers were dipped in rare earth coating solution and dried at 120°C for 5 min. After five times repeating of both dipping and drying, the Ti plates were heated in a muffle oven (550°C for 20 min) for coating pyrolysis. The annealing process as discussed earlier (dipping, drying, and pyrolysis) was repeated 3 times, and finally, the electrodes were annealed at 550°C for 2 h.

2.4. Characterization of Electrodes. The crystal structure of the electrodes was characterized by a Bruker D8 ADVANCE X-ray diffractometer (Germany) with Cu-Kα radiation with an operation voltage of 40 kV and current of 40 mA. A Zeiss Supra 55 instrument was employed to analyze the surface morphologies and EDS of the different electrodes. The electrochemical workstation (CHI 660E, Chenhua Instrument Shanghai Co. Ltd., China) with a conventional three-electrode cell was employed to execute cyclic voltammetry (CV) in the range of 0.0–2.5 V (vs. SCE) at a scan rate of 50 mV s^{-1} in 0.5 M Na_2SO_4 solutions. A platinum sheet was used as a counter electrode, and a saturated calomel electrode (SCE) served as a reference electrode. To characterize service lifetime and to reduce the experimental time, the accelerated life test was conducted in two-electrode system cell. The as-prepared electrodes were applied as the working electrode, and titanium plate as the counter electrode was placed at a 10 mm distance apart under 500 mAcm^{-2} controlled current density. The electrolyte solution 3 M H_2SO_4 was used, and the cell temperature was controlled at 40°C. The deactivated electrodes were assumed when the cell potential reached 10 V.

2.5. Phenol Degradation Test. Electrochemical degradation of phenol was performed in 100 ml glass beakers. For each cell, the as-prepared electrodes (4 cm^2) (2 cm × 2 cm) were used as the anode and the titanium sheet cathodes having the same area were placed at a 10 mm spacing distance. For a degradation test, 80 ml of a phenol solution with a predetermined concentration of 100 mgl^{-1} was placed in the cell with 0.1 M Na_2SO_4 as the electrolyte and the current density was controlled at 30 mAcm^{-2}. The phenol removal rate was found to fit well the pseudofirst-order kinetics, and the degradation rate could be expressed by equation (2). All the electrochemical oxidation processes were carried out at 25°C for 140 min with a magnetic stirrer. The removal of phenol concentrations was determined by the 4-amino antipyrine spectrophotometric method. A UV2200 UV-VIS spectrophotometer (Ocean Optics, Dunedin, FL) was employed to record the absorbance of the liquid samples (1 ml) at the wavelength of 510 nm, which were withdrawn from the electrolytic cell at fixed time

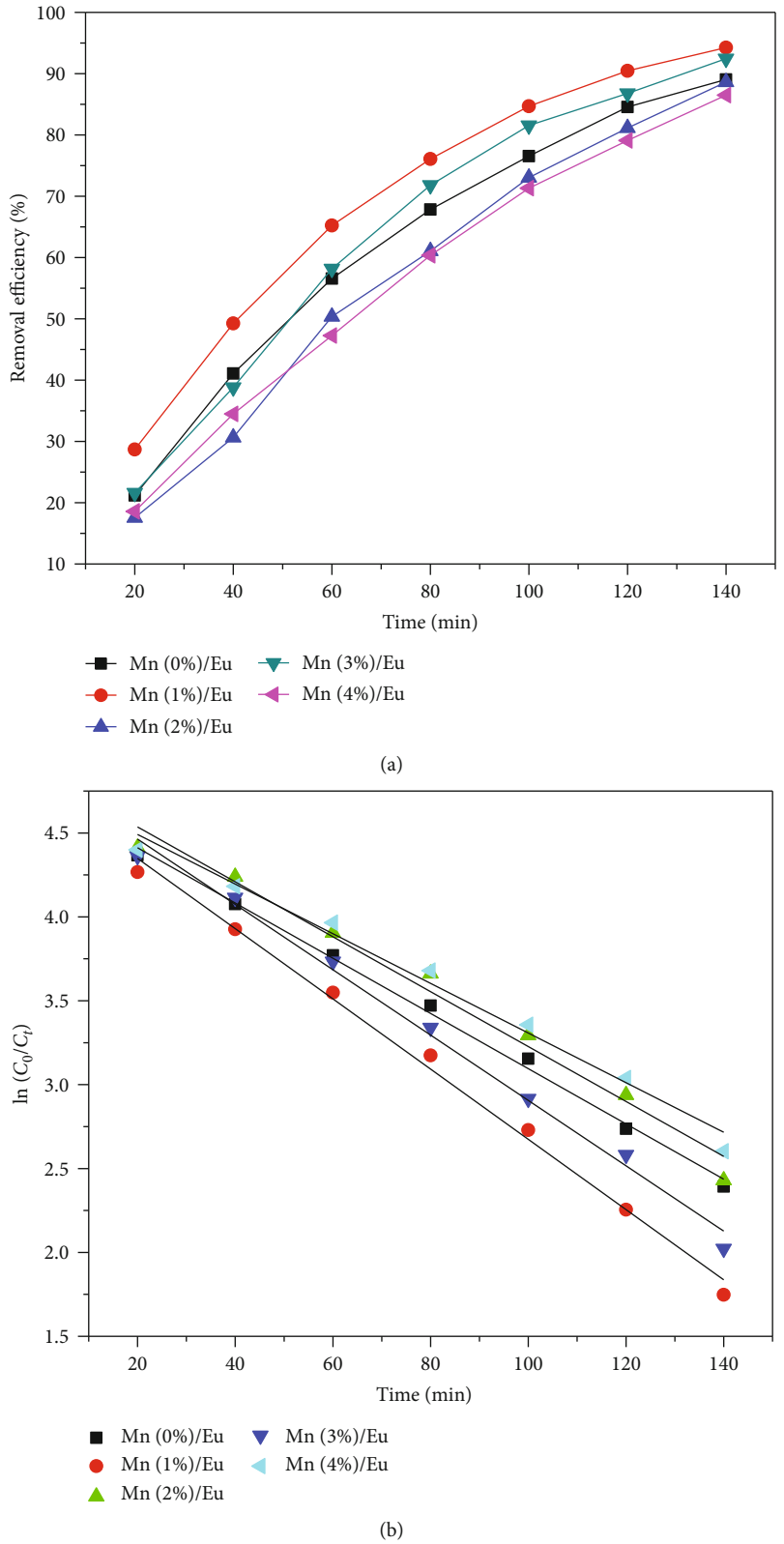

FIGURE 2: Electrochemical degradation performance of phenol with Ti/Mn-Sb-SnO_2/Eu electrodes modified with various Mn contents. (a) Removal efficiency. (b) Kinetic analysis of the curves.

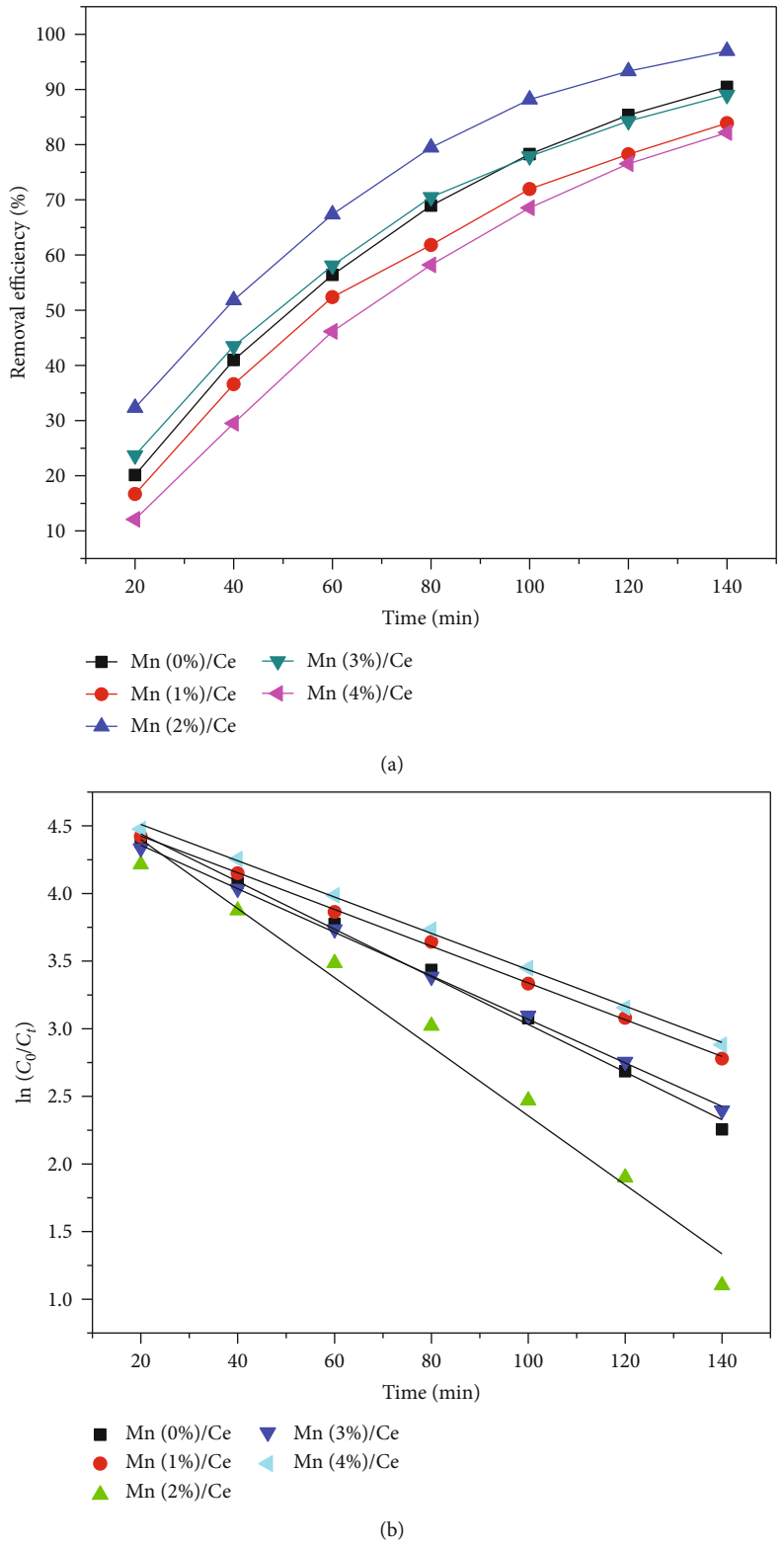

Figure 3: Electrochemical degradation performance of phenol with Ti/Mn-Sb-SnO_2/Ce electrodes modified with various Mn contents. (a) Removal efficiency. (b) Kinetic analysis of the curves.

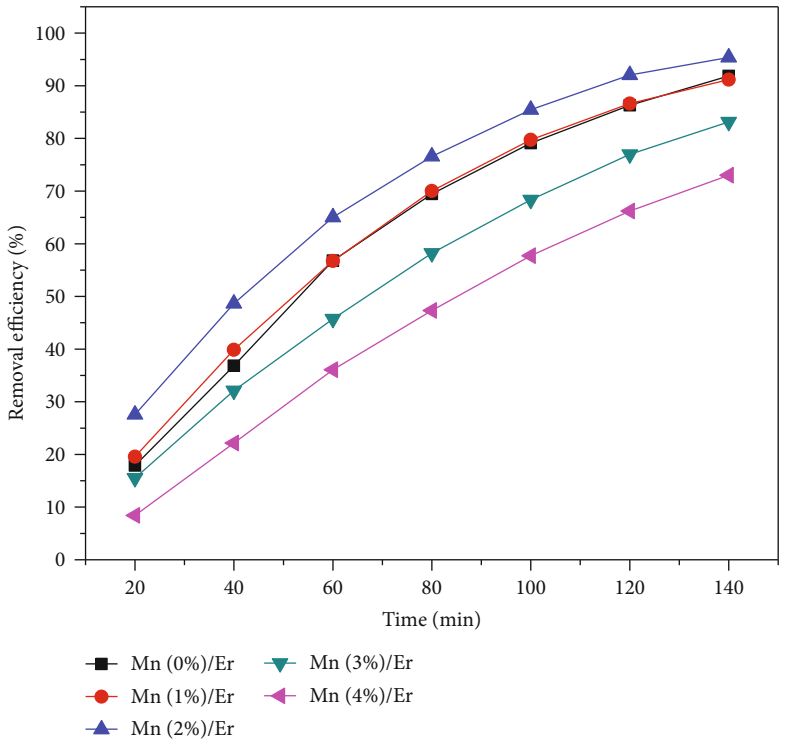

(a)

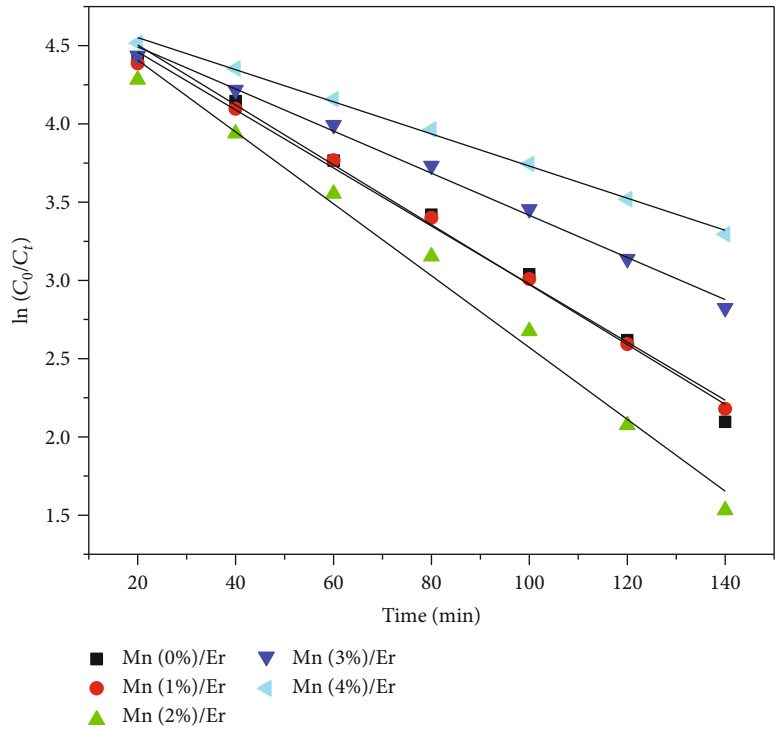

(b)

Figure 4: Electrochemical degradation performance of phenol with Ti/Mn-Sb-SnO_2/Er electrodes modified with various Mn contents. (a) Removal efficiency. (b) Kinetic analysis of the curves.

Table 2: Kinetic parameters of phenol in electrochemical processes by Ti/Mn-Sb-SnO_2/Re electrodes (Er and Ce) modified with various Mn contents.

	Mn (0%)/Er	Mn (1%)/Er	Mn (2%)/Er	Mn (3%)/Er	Mn (4%)/Er
Rate constants (k) (min^{-1})	0.0191	0.0186	0.0230	0.0135	0.0103
R^2	0.9922	0.9961	0.9896	0.9944	0.9973
	Mn (0%)/Ce	Mn (1%)/Ce	Mn (2%)/Ce	Mn (3%)/Ce	Mn (4%)/Ce
Rate constants (k) (min^{-1})	0.0176	0.0136	0.0255	0.0161	0.0134
R^2	0.9956	0.9991	0.9813	0.9991	0.9986

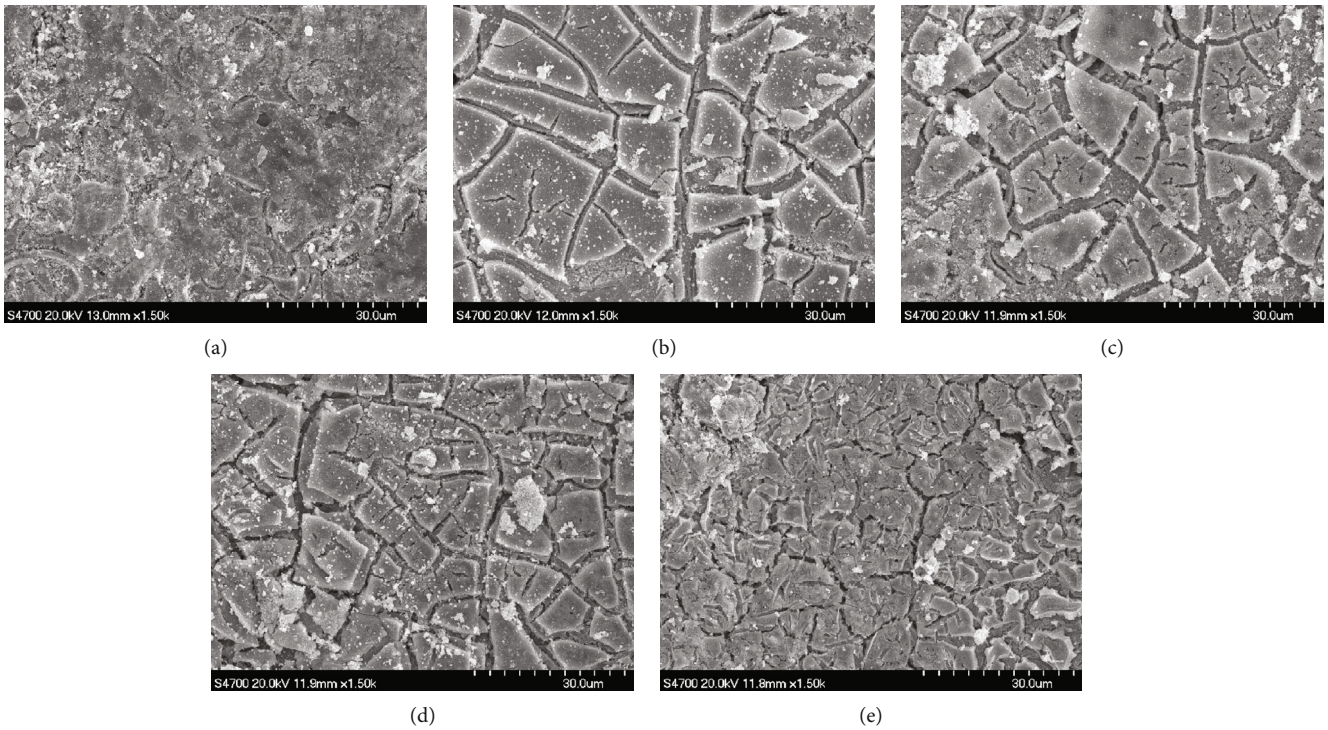

(a) (b) (c) (d) (e)

Figure 5: SEM images of Gd-doped/Ti-Mn-Sb-SnO_2 with (a) Mn (0%), (b) Mn (1%), (c) Mn (2%), (d) Mn (3%), and (e) Mn (4%).

intervals to determine the variation of phenol concentration. The removal efficiency of phenol (η) was calculated as follows:

$$\eta = \frac{C_0 - C}{C_0} \times 100\%, \quad (1)$$

where C_0 and C are the initial and remaining concentrations of phenol, respectively. The concentrations were obtained from the standard curve.

3. Results and Discussion

3.1. Electrochemical Degradation Tests. The electrocatalytic activity of the different rare earth electrodes prepared with various Mn doping interlayer was investigated with degradation experiments (2.3 h electrolysis) by using the phenol solution as a target pollutant. The removal of phenol concentration (95%) can be reduced at a Mn (1%)/Gd electrode (Figure 1(a)), and the rate constant was higher than the other electrodes (Table 1). The removal efficiency (94%) was reached with a Mn- (1%) based Eu-doped electrode (Figure 2(a)). The interlayer doping concentration of Mn (2%) of a Ce electrode removed the phenol up to 97% (Figure 3(a)), and that of an Er electrode was 95% removal efficiency (Figure 4(a)), respectively. These conditions and removal rates were better than the Mn (0%) electrode and the other Mn various concentrations. The phenol removal rates were also fitted with pseudofirst-order kinetics (Tables 1 and 2) and the rate equation for the as shown in eqn.

$$C_t = C_0 e^{-kt}, \quad (2)$$

where C_0 is the initial concentration of phenol, C is the concentration of phenol at given time t, and k is the kinetic rate constant.

Among all of the rare earth electrodes as mentioned above, the kinetic rates were achieved at the Mn (1%) with Gd (Figure 1(b)), and that with Eu electrodes (Figure 2(b))

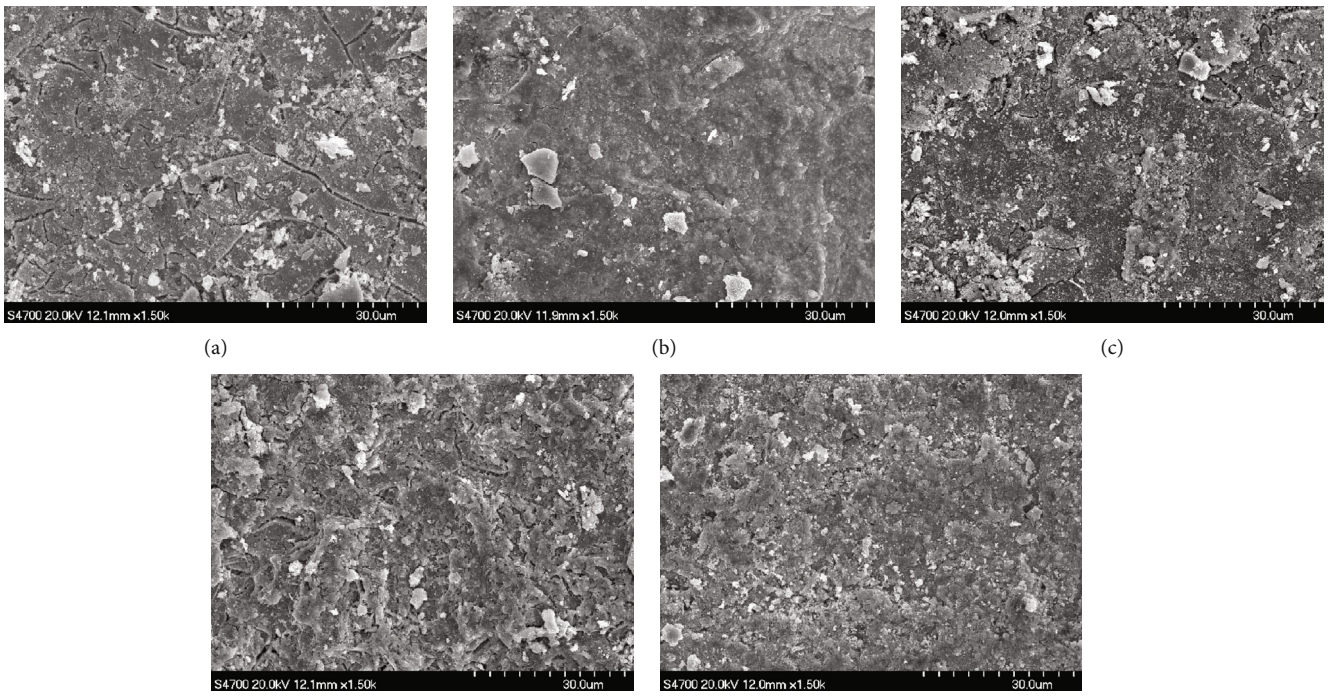

Figure 6: SEM images of Eu-doped/Ti-Mn-Sb-SnO_2 with (a) Mn (0%), (b) Mn (1%), (c) Mn (2%), (d) Mn (3%), and (e) Mn (4%).

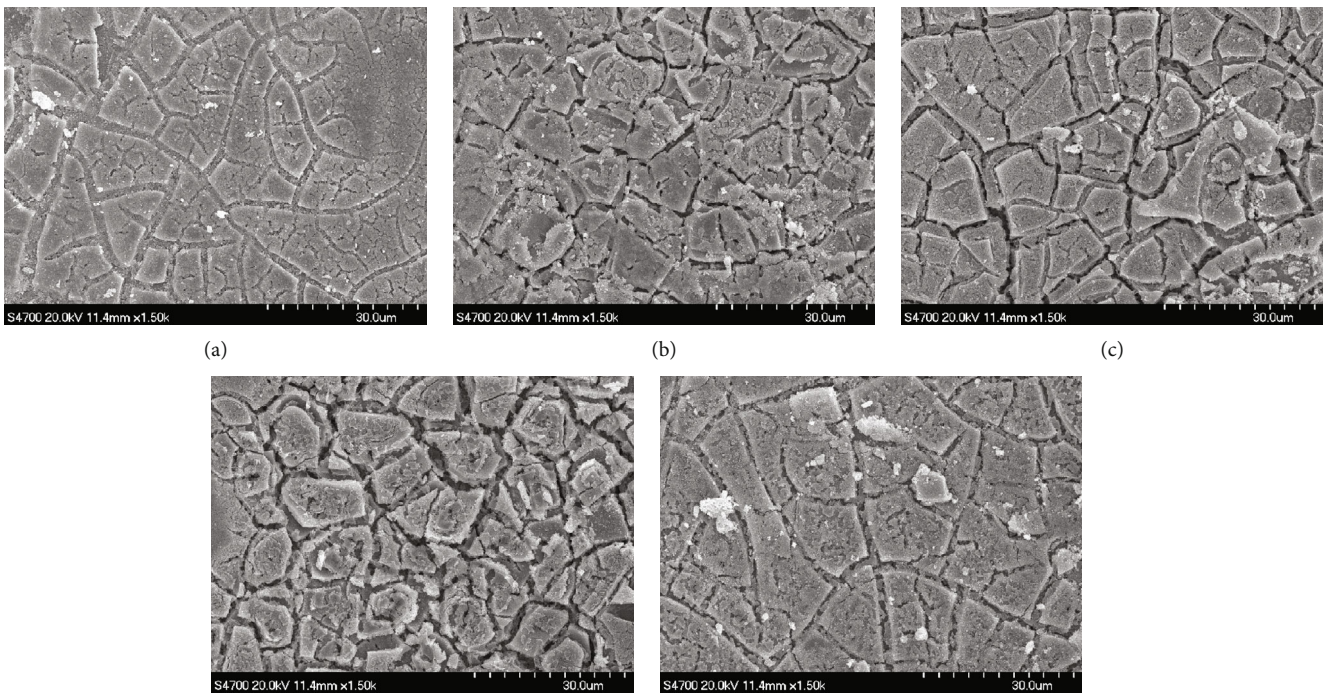

Figure 7: SEM images of Ce-doped/Ti-Mn-Sb-SnO_2 with (a) Mn (0%), (b) Mn (1%), (c) Mn (2%), (d) Mn (3%), and (e) Mn (4%).

were 1.08 times and 1.27 times the rest of Mn (2%)/Ce (Figure 3(b)), and Er electrodes (Figure 4(b)) were 1.45 times and 1.2 times compared with no addition of Mn electrodes. According to the degradation tests, the Mn concentration of 1 mol% and 2 mol% was the proper amount for the inner layer. Therefore, the modified Mn layer-based rare earth electrodes significantly enhance the performance of electrochemical degradation of phenol.

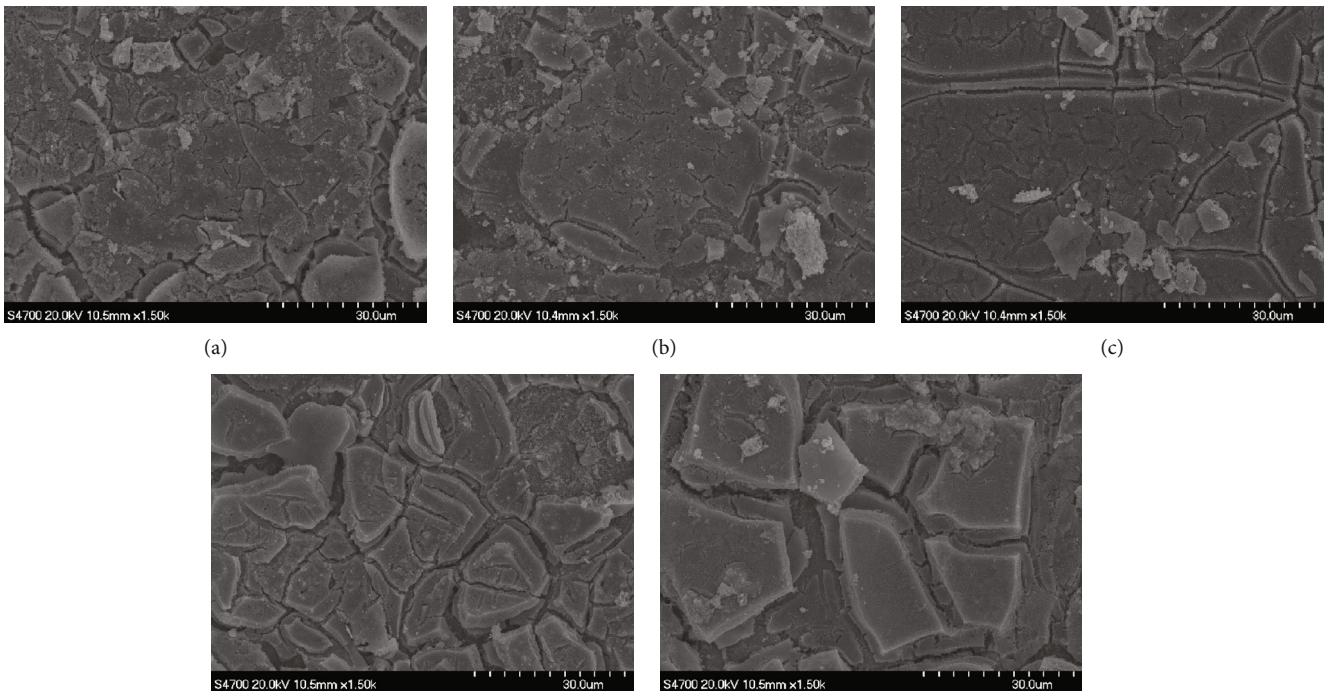

(a) (b) (c)

(d) (e)

Figure 8: SEM images of Er-doped/Ti-Mn-Sb-SnO_2 with (a) Mn (0%), (b) Mn (1%), (c) Mn (2%), (d) Mn (3%), and (e) Mn (4%).

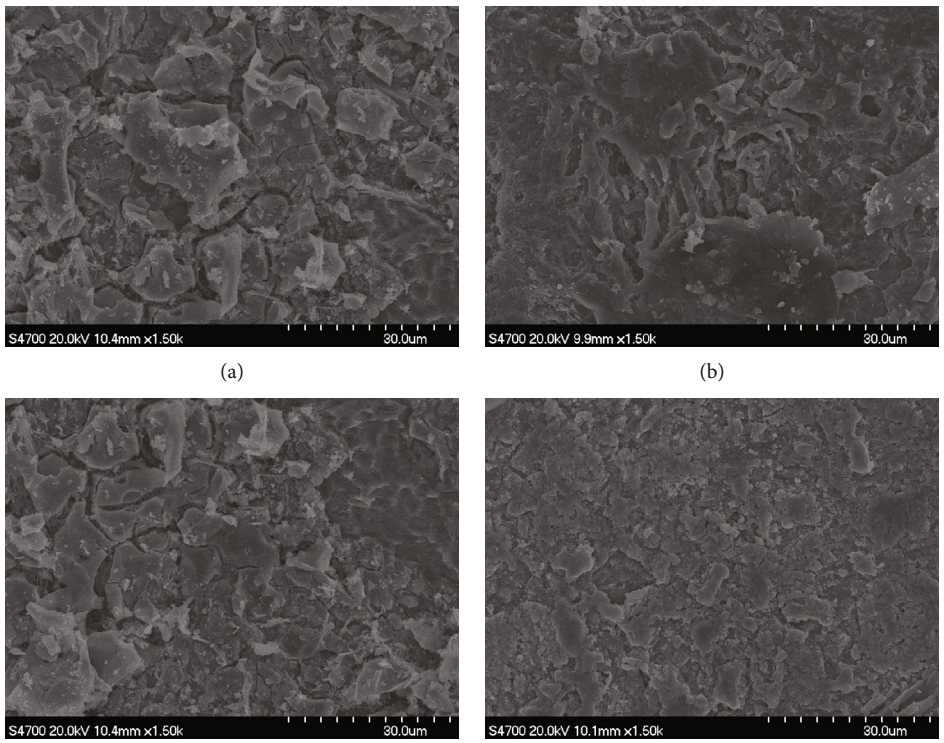

(a) (b)

(c) (d)

Figure 9: SEM images of (a) Gd-doped/Ti-Mn-Sb-SnO_2 with Mn (1%), (b) Eu-doped/Ti-Mn-Sb-SnO_2 with Mn (1%), (c) Ce-doped/Ti-Mn-Sb-SnO_2 with Mn (2%), and Er-doped/Ti-Mn-Sb-SnO_2 with Mn (2%) after 120 min electrolysis.

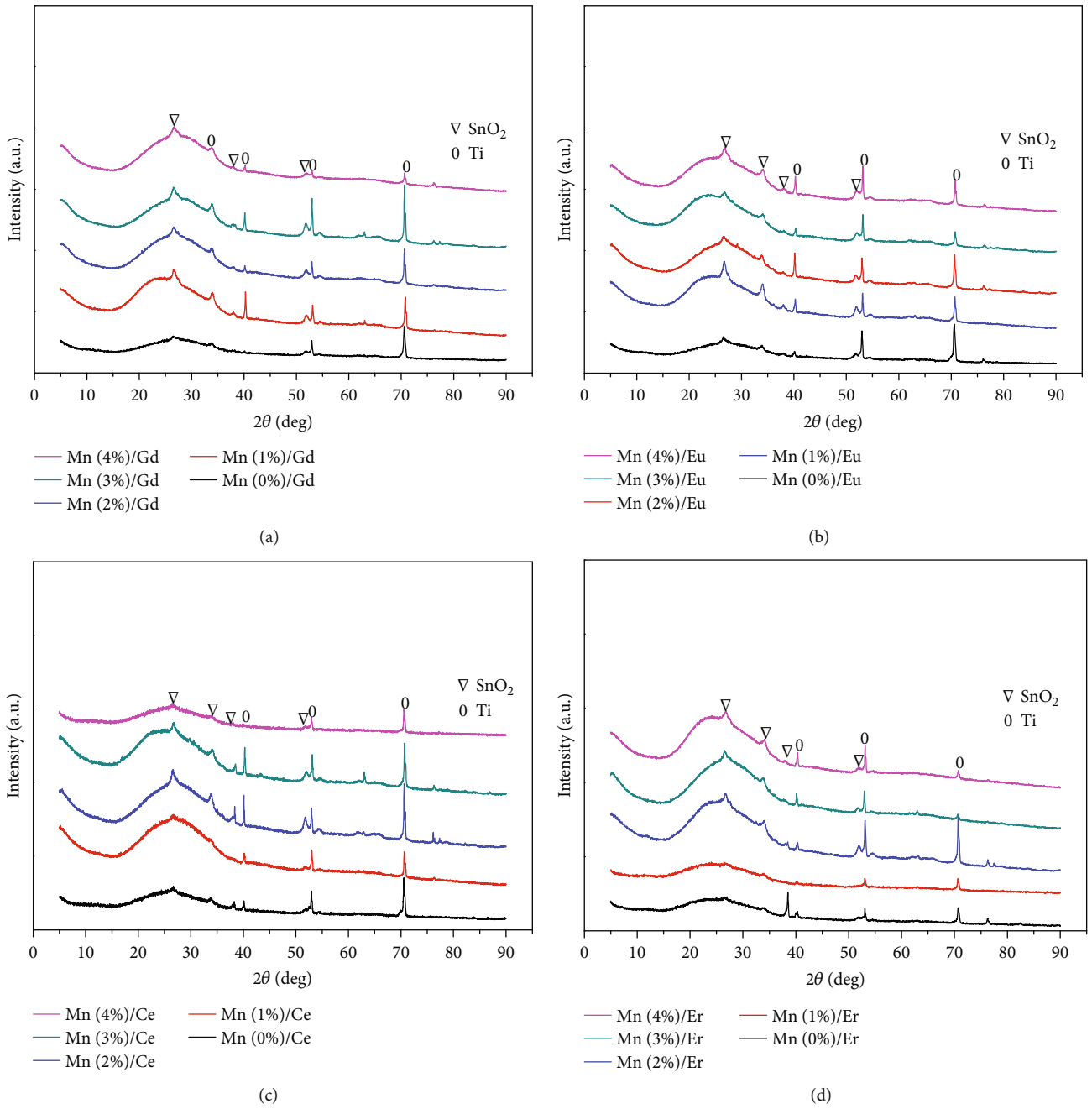

Figure 10: XRD patterns of Ti/Sb-Mn-SnO_2 (0%,1%,2%,3%, and 4%) doped with (a) Gd, (b) Eu, (c) Ce, and (d) Er electrodes.

3.2. Surface Morphology and Structure Analysis. SEM was utilized to characterize the morphology of the rare earth- (Gd, Eu, Ce, and Er) (Re-) doped SnO_2-Sb-Mn anodes as shown in Figures 5–8. All of the images (Figures 5–8) which present the cracked-mud morphology were perceived as the aftereffect of thermal oxidation [20]. Manganese inserts into the Sb-SnO_2 can improve resistance to the thermal stress of coating and construction of a more compact morphological structure which consists of microcracks and agglomerated particles [32]. Figures 9(a)–9(d) observed that the modified electrodes presented a rough structure with good attachments and smaller coating loss after 120 min phenol electrolysis. Formation of a nonconductive TiO_2 layer due to the entering oxygen atoms resulting from the electrolysis process can facilitate change that can favor stripping off the coating layers [21]. The prepared oxide films showed demonstrated a progression of diffraction peaks identified with rutile-type SnO_2 (PDF#41-1445) and Ti (PDF#44-1294) for the majority of the prepared Re-doped Ti/SnO_2-Sb-Mn electrodes including various rare earth and different Mn contents, and the fundamental diffraction peaks were named (Figure 10). The Mn content increased from 1% to 4%; the intensities of the SnO_2 diffraction peaks increased. In any case, the degradation abilities were

Table 3: Coating composition of electrodes (at. %).

Chemical element	Percentage of element			
	Ti/SnO_2-Sb-Mn (1%)/Gd	Ti/SnO_2-Sb-Mn (1%)/Eu	Ti/SnO_2-Sb-Mn (2%)/Ce	Ti/SnO_2-Sb-Mn (2%)/Er
Sn	52.63	42.60	59.09	40.85
Sb	6.20	3.28	4.30	2.56
Mn	0.21	2.29	1.86	0.56
Gd	1.77	0.00	0.00	0.00
Eu	0.00	1.05	0.00	0.00
Ce	0.00	0.00	2.12	0.00
Er	0.00	0.00	0.00	1.31

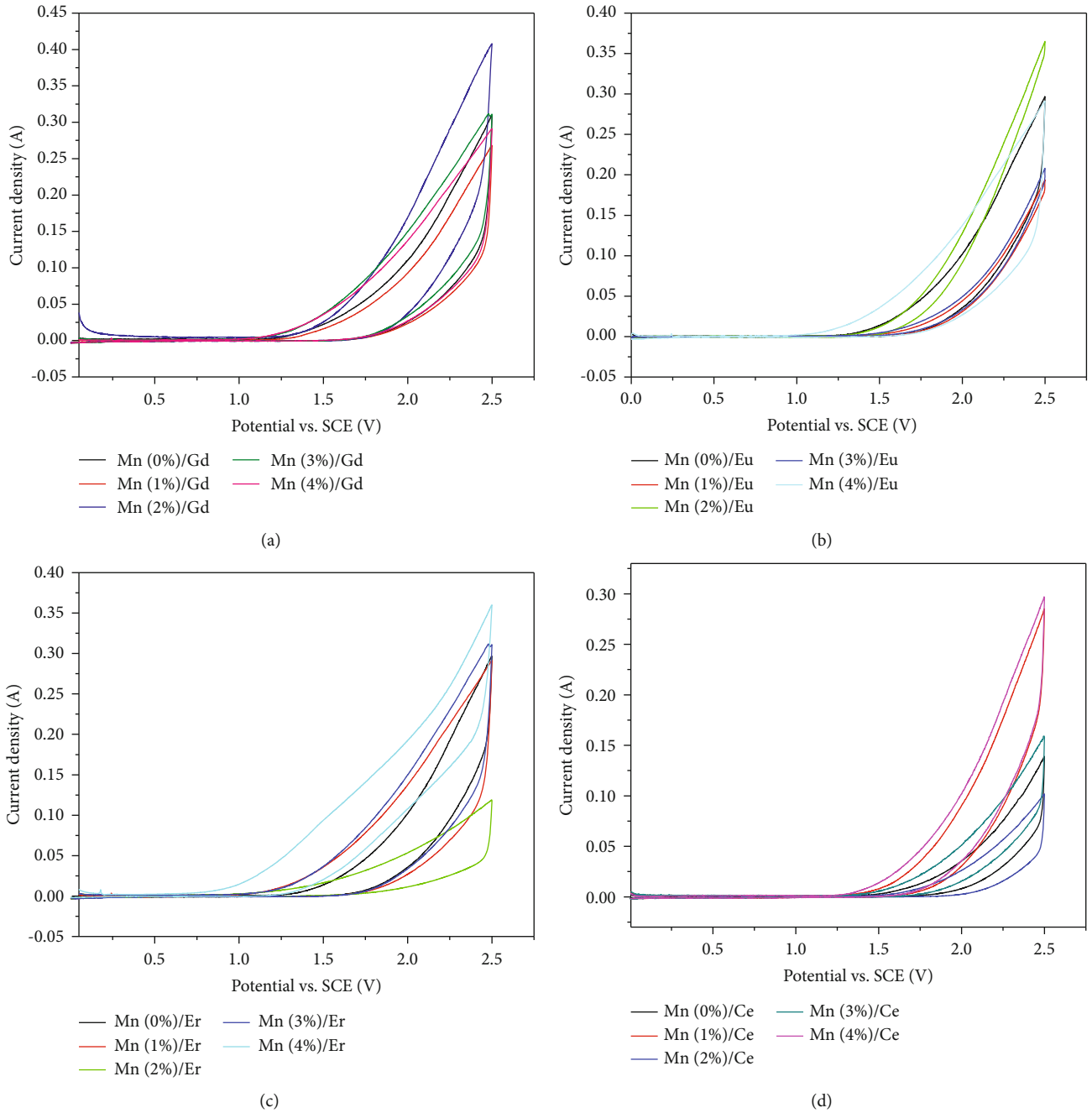

Figure 11: Cyclic voltammetry curves of Ti/SnO_2-Sb-Mn (0%,1%,2%,3%, and 4%) doped with (a) Gd, (b) Eu, (c) Er, and (d) Ce electrodes.

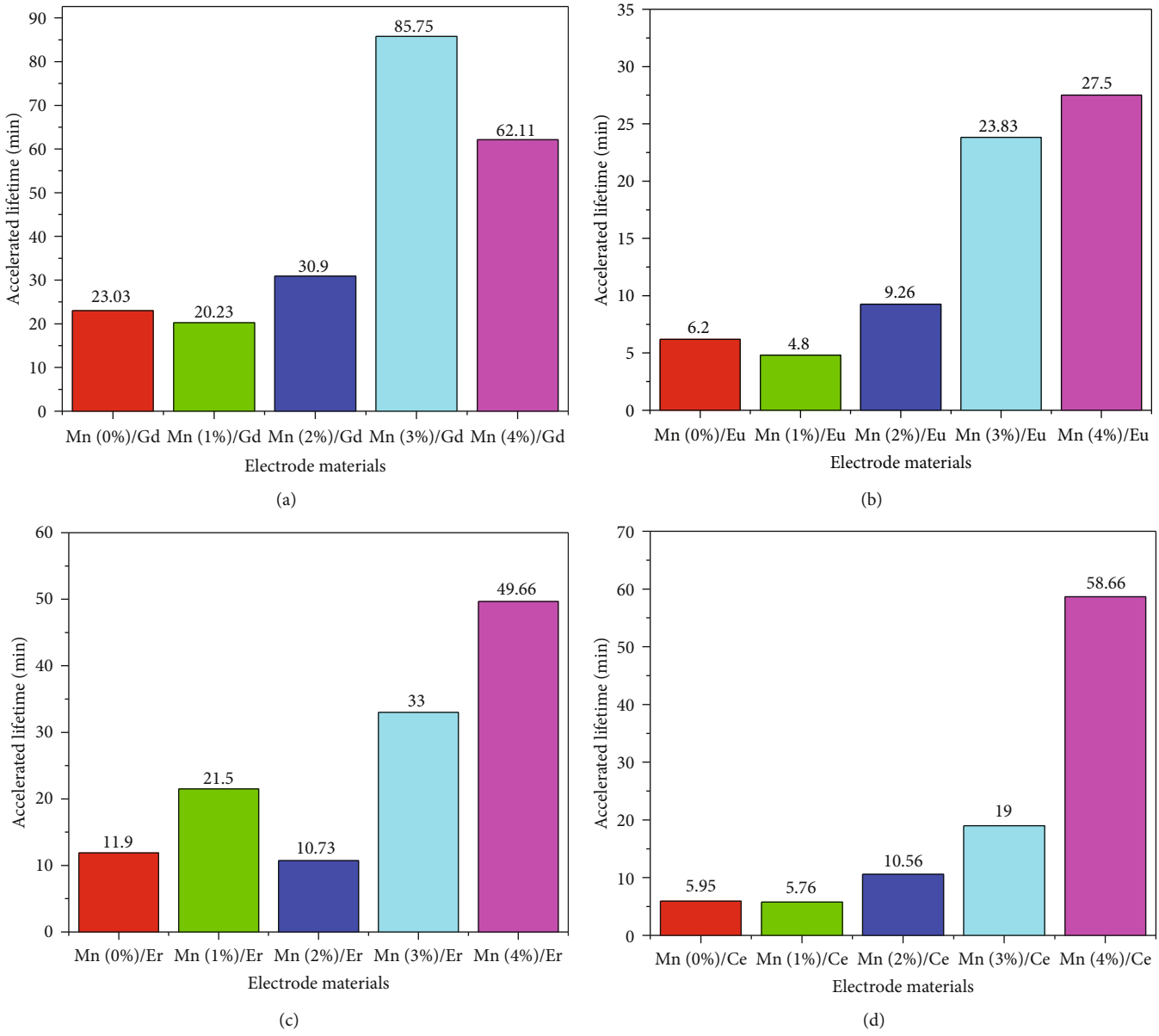

Figure 12: The accelerated service life of prepared (a) Gd, (b) Eu, (c) Er, and (d) Ce electrodes in 3 M H_2SO_4 aqueous solution with a cell temperature of 40°C, performed under a constant current density of 500 mA·cm^{-2}.

decreased with including Mn amount of 1-4% as the result of these intensities increased. Thus, Mn addition of 1% for Gd and Eu and 2% for Ce and Er is ideal for improving the electrocatalytic capacity of all rare earth electrodes without well SnO_2 crystal formation. There are no distinct diffraction peaks of Sb, Mn, and rare earth metal oxides in the XRD spectrums due to either the low doping level or the consolidation of the doping ions into the SnO_2 unit cell. EDS confirmed the contents of Sn, Sb, rare earth (Re), and Mn in the Re-doped SnO_2-Sb-Mn electrodes (Table 3). The expanded Sb concentration in the SnO_2 cross sections is believed to be useful for adsorption of polar molecules and in this manner can upgrade the electroreactant limit of the electrodes [33].

3.3. Cyclic Voltammetry Tests. The high oxygen evolution potential (OEP) of anodes benefits the degradation of phenol, because the OEP can control the formation of $OH^{\cdot}$ and O in the electrolyte during the electrolysis processes from forming oxygen and produced more and broaden the lifetime of the hydroxyl radicals on the anode [24], which is good to expand the rate of removal and the current efficiency [34]. Figure 11 represents the CV curves of various electrodes in 0.5 M Na_2SO_4 supporting electrolyte. As per the CV curves, the edge potential for oxygen evolution lies in Mn (1%) of Gd (2.0329 V) and that of Eu (2.2430 V), for Mn (2%) Ce (2.4915 V) and Mn (2%) Er (2.3788 V), respectively, higher than without the Mn/Re-doped electrode.

3.4. Accelerated Life Tests. Not only the electrocatalytic activity but also sufficient electrode stability is necessary for the performance of the electrodes. The current density, temperature, and pH of the electrolyte are mainly related to the actual service lifetime. In the actual condition, the applied current density is low and difficult to evaluate the actual service life time. To ensure the best durable performance and reduce the test time, the accelerated lifetime test has been applied to evaluate the whole service life of the electrodes. An empirical relationship between the accelerated service life (T_1) and the actual service life (T_2) was proposed, which could assess the actual service life of [35].

$$T_2 = \left(\frac{J_2}{J_1}\right)^n T_1, \tag{3}$$

where n is a constant often equal to 2, J_1 is the actual current density, and J_2 is the accelerated current density. Figure 12 demonstrates that the accelerated life test results and the cell voltage varied with time for the prepared electrodes. The increased service life was observed in the electrode content with Mn (3% and 4%) compared with other electrodes. The rare earth Gd and Eu with interlayer Mn (2%) electrodes show that the service life is higher than those electrodes without the Mn layer but at Mn (1%) are lower as shown in Figures 12(a) and 12(b). Although the Mn (2%)/Ce electrode has great service life, the Mn (1%)/Ce was not having that condition compared with the Mn (0%)/Ce electrode (Figure 12(d)). As mentioned in Figure 12(c), the high life of the electrode was watched at the Mn (1%)/Er by comparing with the Mn (0%)/Er and Mn (2%)/Er electrodes. The four mechanisms can cause the electrode deactivation: metal base passivation, coating detachment, coating consumption, and mechanical damage [36]. The more significant explanation is that electrolyte responds with the Ti substrate and structures a layer of inactive film in the wake of penetrating the middle layer [37].

4. Conclusions

The distinctive molar proportions of Sn/Mn and the doping influence of rare earth Gd, Eu, Ce, and Er were researched to uncover their impacts on the catalytic performance of the electrodes. The accelerated life test outcomes demonstrated that the service life was significantly higher in the Mn (3% and 4%) of all prepared rare earth electrodes than that of others. The best degradation rate of phenol was found in the Mn (1%) and (2%) doped Re electrodes compared with other Mn adding and no adding Mn-doped rare earth electrodes. XRD analysis investigation demonstrated the crystalline structure of the SnO_2 coating on the surface of all the synthesized electrodes. However, due to the consolidation of the doping ions (Sb, Mn, and Re) into the SnO_2 structure, it was unrealistic to recognize them through XRD. But EDS affirmed the inclusion of those doping elements. Based on these experimental results, the proper contents of Mn added between the substrate and the rare earth outer layer can enhance the performance of the electrodes.

Data Availability

The data used to support the findings of this study are included within the article.

Conflicts of Interest

Zenghe Li, corresponding author, declares that there is no conflict of interests regarding the publication of this paper.

Acknowledgments

This work was supported by Zenghe Li as a funder, corresponding author at Beijing Key Laboratory of Environmentally Harmful Chemical Analysis, College of Chemistry, Beijing University of Chemical Technology, Beijing, 100029, China.

References

[1] W. E. Luttrell, "Toxic tips: phenol," *Chemical Health and Safety*, vol. 10, no. 5, pp. 20-21, 2003.

[2] H. Awad and N. A. Galwa, "Electrochemical degradation of Acid Blue and Basic Brown dyes on Pb/PbO2 electrode in the presence of different conductive electrolyte and effect of various operating factors," *Chemosphere*, vol. 61, no. 9, pp. 1327–1335, 2005.

[3] J. M. Dickhout, J. Moreno, P. M. Biesheuvel, L. Boels, R. G. H. Lammertink, and W. M. de Vos, "Produced water treatment by membranes: a review from a colloidal perspective," *Journal of Colloid and Interface Science*, vol. 487, pp. 523–534, 2017.

[4] C. Petrier and A. Francony, "Ultrasonic waste-water treatment: incidence of ultrasonic frequency on the rate of phenol and carbon tetrachloride degradation," *Ultrasonics Sonochemistry*, vol. 4, no. 4, pp. 295–300, 1997.

[5] B. Tuleva, N. Christova, B. Jordanov, B. Nikolova-Damyanova, and P. Petrov, "Naphthalene degradation and biosurfactant activity by Bacillus cereus 28BN," *Zeitschrift für Naturforschung C*, vol. 60, no. 7-8, pp. 577–582, 2005.

[6] A. Pawar, "Biological degradation of naphthalene: a new era," *Journal of Bioremediation & Biodegradation*, vol. 4, no. 7, pp. 1–5, 2013.

[7] C. Ania, B. Cabal, C. Pevida et al., "Removal of naphthalene from aqueous solution on chemically modified activated carbons," *Water Research*, vol. 41, no. 2, pp. 333–340, 2007.

[8] R. K. Goel, J. R. Flora, and J. Ferry, "Mechanisms for naphthalene removal during electrolytic aeration," *Water Research*, vol. 37, no. 4, pp. 891–901, 2003.

[9] S. Garcia-Segura, M. M. S. G. Eiband, J. V. de Melo, and C. A. Martínez-Huitle, "Electrocoagulation and advanced electrocoagulation processes: a general review about the fundamentals, emerging applications and its association with other technologies," *Journal of Electroanalytical Chemistry*, vol. 801, pp. 267–299, 2017.

[10] M. R. Santos, M. O. Goulart, J. Tonholo, and C. L. Zanta, "The application of electrochemical technology to the remediation of oily wastewater," *Chemosphere*, vol. 64, no. 3, pp. 393–399, 2006.

[11] G. Chen, "Electrochemical technologies in wastewater treatment," *Separation and Purification Technology*, vol. 38, no. 1, pp. 11–41, 2004.

[12] J. H. B. Rocha, M. M. S. Gomes, N. S. Fernandes, D. R. da Silva, and C. A. Martínez-Huitle, "Application of electrochemical oxidation as alternative treatment of produced water generated by Brazilian petrochemical industry," *Fuel Processing Technology*, vol. 96, pp. 80–87, 2012.

[13] S. Trasatti, "Electrocatalysis: understanding the success of DSA®," *Electrochimica Acta*, vol. 45, no. 15-16, pp. 2377–2385, 2000.

[14] C. Comninellis, "Electrocatalysis in the electrochemical conversion/combustion of organic pollutants for waste water treatment," *Electrochimica Acta*, vol. 39, no. 11-12, pp. 1857–1862, 1994.

[15] P. R. F. da Costa, D. R. da Silva, C. A. Martínez-Huitle, and S. Garcia-Segura, "Fuel station effluent treatment by electrochemical technology," *Journal of Electroanalytical Chemistry*, vol. 763, pp. 97–103, 2016.

[16] G. Wang, L. Zhang, and J. Zhang, "A review of electrode materials for electrochemical supercapacitors," *Chemical Society Reviews*, vol. 41, no. 2, pp. 797–828, 2012.

[17] A. M. Polcaro, S. Palmas, F. Renoldi, and M. Mascia, "On the performance of Ti/SnO2 and Ti/PbO2 anodesin electrochemical degradation of 2-chlorophenolfor wastewater treatment," *Journal of Applied Electrochemistry*, vol. 29, no. 2, pp. 147–151, 1999.

[18] M. Li, C. Feng, W. Hu, Z. Zhang, and N. Sugiura, "Electrochemical degradation of phenol using electrodes of Ti/RuO(2)-Pt and Ti/IrO(2)-Pt," *Journal of Hazardous Materials*, vol. 162, no. 1, pp. 455–462, 2009.

[19] X.-y. Li, Y.-h. Cui, Y.-j. Feng, Z.-m. Xie, and J.-D. Gu, "Reaction pathways and mechanisms of the electrochemical degradation of phenol on different electrodes," *Water research*, vol. 39, no. 10, pp. 1972–1981, 2005.

[20] Y.-H. Cui, Y.-J. Feng, and Z.-Q. Liu, "Influence of rare earths doping on the structure and electro-catalytic performance of Ti/Sb–SnO2 electrodes," *Electrochimica Acta*, vol. 54, no. 21, pp. 4903–4909, 2009.

[21] Z. Zhang, Q. Q. Sun, and Y. P. Si, "Degradation properties of Ti/Sb-SnO₂ electrodes containing different intermediate layers for phenol," *Materials Science Forum*, vol. 743-744, pp. 420–426, 2013.

[22] H. An, Q. Li, D. Tao et al., "The synthesis and characterization of Ti/SnO2–Sb2O3/PbO2 electrodes: the influence of morphology caused by different electrochemical deposition time," *Applied Surface Science*, vol. 258, no. 1, pp. 218–224, 2011.

[23] Y.-q. Wang, B. Gu, and W.-l. Xu, "Electro-catalytic degradation of phenol on several metal-oxide anodes," *Journal of Hazardous Materials*, vol. 162, no. 2-3, pp. 1159–1164, 2009.

[24] B. Correa-Lozano, C. Comninellis, and A. De Battisti, "Service life of Ti/SnO2–Sb2O5 anodes," *Journal of Applied Electrochemistry*, vol. 27, no. 8, pp. 970–974, 1997.

[25] L. Junfeng, Y. Feng, J. Lv, and H. Ding, "Enhancing service life of SnO2 electrode by introducing an interlayer containing Mn element," *Chinese Journal of Materials Research*, vol. 22, no. 6, pp. 593–598, 2009.

[26] H. You, Y. H. Cui, Y. J. Feng, J. F. Liu, and W. M. Cai, "Preparation and investigation of Ti-based SnO2 electrode with an inter layer containing Co element," *Materials Science and Technology*, vol. 12, no. 3, pp. 230–233, 2004.

[27] X. Chen, F. Gao, and G. Chen, "Comparison of Ti/BDD and Ti/SnO2?Sb2O5 electrodes for pollutant oxidation," *Journal of Applied Electrochemistry*, vol. 35, no. 2, pp. 185–191, 2005.

[28] A. Trovarelli, "Catalytic properties of ceria and CeO2-containing materials," *Catalysis Reviews*, vol. 38, no. 4, pp. 439–520, 1996.

[29] H. He, H. X. Dai, and C. T. Au, "Defective structure, oxygen mobility, oxygen storage capacity, and redox properties of RE-based (RE = Ce, Pr) solid solutions," *Catalysis Today*, vol. 90, no. 3-4, pp. 245–254, 2004.

[30] S.-Y. Al, J.-Q. Li, L.-P. Li, H.-Q. Peng, Y. Yang, and L.-T. Jin, "Electrochemical deposition and properties of nanometer-structure Ce-doped lead dioxide film electrode," *Chinese Journal of Chemistry*, vol. 23, no. 1, pp. 71–75, 2005.

[31] Y. Feng and X. Y. Li, "Electro-catalytic oxidation of phenol on several metal-oxide electrodes in aqueous solution," *Water Research*, vol. 37, no. 10, pp. 2399–2407, 2003.

[32] C. Shao and Guangdong Research Institute of Rare-Metal, "Performance of manganese and antimony co-doping tin dioxide anodes prepared at different temperatures," *International Journal of Electrochemical Science*, vol. 14, no. 1, pp. 126–136, 2019.

[33] D. He and S.-i. Mho, "Electrocatalytic reactions of phenolic compounds at ferric ion co-doped SnO2:Sb5+ electrodes," *Journal of Electroanalytical Chemistry*, vol. 568, pp. 19–27, 2004.

[34] L. Zhang, L. Xu, J. He, and J. Zhang, "Preparation of Ti/SnO2-Sb electrodes modified by carbon nanotube for anodic oxidation of dye wastewater and combination with nanofiltration," *Electrochimica Acta*, vol. 117, pp. 192–201, 2014.

[35] X. Chen and G. Chen, "Stable Ti/RuO2–Sb2O5–SnO2 electrodes for O2 evolution," *Electrochimica Acta*, vol. 50, no. 20, pp. 4155–4159, 2005.

[36] G. N. Martelli, R. Ornelas, and G. Faita, "Deactivation mechanisms of oxygen evolving anodes at high current densities," *Electrochimica Acta*, vol. 39, no. 11-12, pp. 1551–1558, 1994.

[37] C. Xin, H.-j. Guo, S.-l. Luo, Z.-x. Wang, and X.-h. Li, "Effect of SnO2 intermediate layer on performance of Ti/SnO2/MnO2 electrode during electrolytic-manganese process," *Transactions of Nonferrous Metals Society of China*, vol. 27, no. 6, pp. 1417–1422, 2017.